https://doi.org/10.5194/egusphere-2026-82
Preprint. Discussion started: 30 January 2026

The six-year cycle in atmospheric angular momentum: robustness, zonal-wind structure, and implications for Earth rotation

Julia Pfeffer[1], Anny Cazenave[2*], Rodrigo Abarca-del-Rio[3], Véronique Dehant[4], Mioara Mandea[5], Severine Rosat[6] and Nicolas Gillet[7]

[1] Magellium, 1 rue Arianne, 31520, Ramonville-saint-Agne, France

[2] Laboratoires d'Etudes en Géophysique et Océanographie Spatiale, Université de Toulouse, 14 avenue Édouard Belin, 31401 Toulouse Cedex 9, France

[3] Departamento de Geofísica, Universidad de Concepción, Concepción, Chile

[4] Université catholique de Louvain (UCLouvain), Earth and Life Institute, Belgium & Royal Observatory of Belgium, Avenue Circulaire 3, Brussels, Belgium

[5] Centre National d'Etudes Spatiales, 2 Place Maurice Quentin, 75039, Paris, France

[6]Institut Terre & Environnement de Strasbourg, 5 rue René Descartes, Strasbourg, France

[7]Univ. Grenoble Alpes, Univ. Savoie Mont Blanc, CNRS, IRD, Univ. Gustave Eiffel, ISTerre, Grenoble, 38000, France

*Corresponding author (anny.cazenave@univ-tlse.fr), anny.cazenave@gmail.com

https://doi.org/10.5194/egusphere-2026-82
Preprint. Discussion started: 30 January 2026

Abstract

Variability near a 6-yr period has been reported in the length of day, motions within the Earth's fluid core, several climatic parameters, and atmospheric angular momentum. Here we demonstrate the robustness of a quasi-6-yr oscillation in atmospheric angular momentum using several independent atmospheric reanalysis products over 1980–2020. This signal is highly significant, consistent across datasets, and accounts for up to about 25% of atmospheric angular momentum variance at interannual time scales. Its expression in the atmospheric zonal wind circulation exhibits a coherent vertical structure throughout the troposphere, with maximum amplitudes near the tropopause in the tropical belt. In addition, the 6-yr oscillation in zonal winds is in phase across from southern to northern latitudes. This structure distinguishes the 6-yr signal from the annual cycle and from ENSO-related variability, and points to a large-scale, organized component of the atmospheric circulation, consistent with alternating phases of weaker and stronger atmospheric super-rotation relative to the solid Earth. While the origin of the length-of-day 6-yr cycle is relatively well established and attributed to exchange of angular momentum from the core to the mantle, the process underlying the 6-yr variability in the zonal wind circulation remains to be elucidated.

1. Introduction

At interannual time scale, an oscillation of about 6-yr period and amplitude of ~0.1 ms, has been detected in the length of day (LOD), initially by Vondrak (1997) and further confirmed by numerous studies (e.g., Abarca de Rio et al., 2000; see Pfeffer et al., 2023, for a review). The 6-yr cycle in LOD has been further attributed to the angular momentum exchange between the fluid outer core and the Earth's mantle, either through electromagnetic (e.g., Gillet et al., 2010, 2017) or gravitational coupling (e.g., Mound and Buffett, 2003, 2006). The hypothesis of a deep interior origin of the LOD 6-yr cycle is further supported by the agreement between core flow model predictions for LOD and LOD observations in terms of period, phase, and amplitude (e.g., Finlay et al., 2023; Istas et al., 2023; Rosat and Gillet, 2023). Beyond the solid Earth, recent studies have shown that the atmospheric angular momentum (AAM) also displays a coherent 6-yr cycle that is in phase opposition with that of the LOD (Chen et al., 2019; Rekier et al., 2022; Pfeffer et al., 2023). In addition, variability with a similar periodicity has also been

https://doi.org/10.5194/egusphere-2026-82
Preprint. Discussion started: 30 January 2026

reported in several climatic parameters (Pfeffer et al., 2023), although the physical pathways linking these components remain incompletely understood (Cazenave et al., 2025).

Despite growing evidence for a six-year signal in atmospheric angular momentum (AAM), the role of the atmosphere circulation in this variability remains unclear. In particular, It is not yet known how it is expressed within the zonal circulation that carries the atmospheric angular momentum. Addressing these diagnostic aspects is essential for interpreting the atmospheric contribution to 6-yr variability in AAM and its relationship with LOD variations.

The purpose of the present study is to investigate the characteristics if the 6-yr cycle in the zonal circulation of the atmosphere. Using wind data from an atmospheric reanalysis, we analyze the vertical structure of the 6-yr cycle across tropospheric altitudes and its organization across latitudes and time. The zonal-wind signature of the 6-yr cycle is compared with other sources of interannual wind variability, including annual, ENSO-related fluctuations, and other interannual fluctuations, to highlight similarities and differences in their spatial and vertical characteristics. Next we revisit the presence and robustness of a quasi-6-yr cycle in the atmospheric angular momentum using several independent atmospheric reanalysis products. Finally, we examine the relationship between the 6-yr variability in AAM and LOD, separating mass and motion contributions, and assessing the effect of removing the atmospheric signal from LOD. We then discuss the resulting residual variability in the context of existing estimates of core angular momentum, always focusing on observational constraints rather than detailed dynamical attribution.

2. Data and Methods

The different datasets used in this study are described below.

Zonal wind data and AAM

Zonal-wind fields were extracted from the ERA-5 atmospheric reanalysis (Hersbach et al., 2020) at pressure levels between 1000 hPa and 1 hPa. Monthly means were interpolated to a regular 1° × 1° grid using the conservative xESMF algorithm (Zhuang et al., 2024). The AAM is estimated from three atmospheric reanalysis products: NCEP/NCAR (Zhou et al., 2006), MERRA-2 (Gelaro et al., 2017), and ERA-Interim (Dee et al., 2011). The ERA-Interim AAM functions are part of the consistent excitation series distributed by the German Research Center for Geosciences (GFZ) (Dobslaw et al., 2010). Both motion and mass terms are taken into account.

https://doi.org/10.5194/egusphere-2026-82
Preprint. Discussion started: 30 January 2026

LOD

LOD variations are taken from the EOP C04 combined series (Bizouard et al., 2019) provided by the International Earth Rotation and Reference Systems Service (IERS), which combines VLBI, SLR, GNSS, and DORIS observations, and is corrected for tidal effects, following IERS Conventions 2010 (Petit and Luzum, 2010).

Core angular momentum

Core angular momentum (CAM) predictions rely on an ensemble of core flow models developed by Gillet et al. (2022). The core surface flow is inferred from the radial component of the induction equation at the core surface (see eq. 7 in Gillet et al., 2022). The geomagnetic secular variation is that provided by the COV-OBS-x2 (Huder et al., 2020) and CHAOS-7 (Finlay et al., 2020) models, both of which combine geomagnetic observations from ground observatories and low Earth orbit satellites (i.e. Swarm, CryoSat-2, CHAMP, SAC-C, and Ørsted). An ensemble of 50 realizations has been calculated using the pygeodyn data assimilation algorithm (Huder et al. 2019; Istas et al. 2023), allowing to account for uncertainties in the geomagnetic field observations. The ensemble trajectories are constrained by spatiotemporal statistics derived from geodynamo simulations (Gillet et al., 2019).

Other data

The Multivariate ENSO Index (MEI v2) (Wolter and Timlin, 1998) from NOAA was used to describe El Niño–Southern Oscillation variability.

Data processing

All datasets were analyzed over January 1980–December 2020, except for one reanalysis (MERRA-2) available only up to 2016. The term “6-yr cycle” is used here generically, acknowledging that the period may vary within 5.1–7.2 years, as constrained by the Rayleigh criterion (Godin, 1972) for a 36-year-long record. A fifth-order Butterworth band-pass filter (5.2–7 years) was applied to all time series to isolate the 6-yr component, accounting for the spectral dispersion around the peak rather than a single dominant period. This filter provides a flat frequency response within the passband while suppressing higher- and lower-frequency variations. Before spectral analysis, each series was detrended and its annual and semi-annual components removed to suppress seasonal variability. Spectral power was computed with the Lomb–Scargle periodogram (VanderPlas, 2018). The significance of peaks was tested against 10,000 red-noise simulations generated through a Monte Carlo approach preserving the

https://doi.org/10.5194/egusphere-2026-82
Preprint. Discussion started: 30 January 2026

observed autocorrelation and variance (Pfeffer et al., 2023). For each significant peak, amplitude and phase were obtained by fitting a sinusoid of the detected period using ordinary least squares. Confidence levels at 95% for instance correspond to the power levels at which only 5% of the 10,000 PSDs of red-noise realizations lie below, meaning that peaks above that level would have <5% chance to be only due to red noise.

3. Characteristics of the six-year cycle in the atmospheric zonal wind circulation

We have analyzed the behavior of the 6-yr cycle of the ERA-5 zonal winds as a function of altitude and latitude (averaging the wind data across longitude).
Spectral analyses of zonal-wind speeds (data globally averaged over the Earth's surface) reveal a significant (> 95 % CL) 6-yr cycle throughout the troposphere and lower stratosphere, as shown in Figure 1. We observe a significant peak around 5.6 years from the surface (1000 hPa) to the tropopause (100-200 hPa), but it disappears in the lower stratosphere (10 hPa) where a peak at 2.3 years, likely the stratospheric biennial oscillation, is well visible. From Figure 1 we also note a peak around 11 years, particularly strong in the lower troposphere. This peak is likely related to the solar cycle.

https://doi.org/10.5194/egusphere-2026-82
Preprint. Discussion started: 30 January 2026

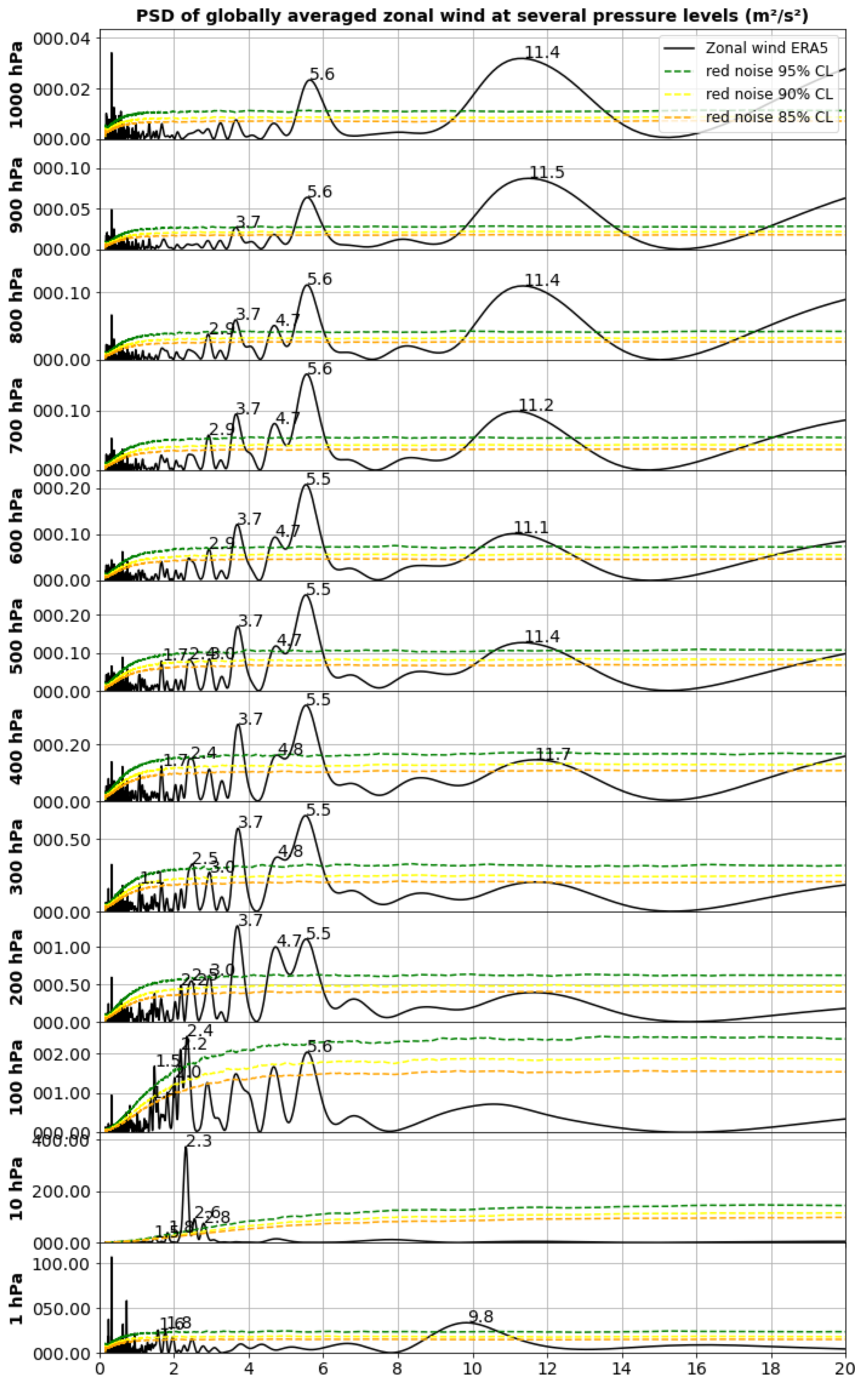

https://doi.org/10.5194/egusphere-2026-82
Preprint. Discussion started: 30 January 2026

Figure 1: Power Spectral Densities (PSD) of globally averaged zonal winds (using the ERA5 atmospheric reanalysis) at several pressure levels. The colored dashed curves represent the confidence levels estimated with red noise assumption.

In Table 1, we present periods and associated confidence levels of the globally averaged zonal wind speed, as well as amplitude (in m s^{-1}) and phase for different altitudes (expressed as pressure levels in hPa) within the troposphere and lower stratosphere.

Table 1: Six-year cycle in globally averaged zonal-wind speed (ERA5, 1980–2020). Periods correspond to spectral maxima nearest 6 years.

Pressure level (hPa)	**Period (yrs)**	**Confidence Level (%)**	**Amplitude (m/s)**	**Phase (°)**
1000	5.64	99.72	0.036	1
900	5.57	99.90	0.059	0
800	5.57	99.98	0.078	1
700	5.57	99.98	0.094	0
600	5.54	100.00	0.106	-3
500	5.54	99.94	0.117	-7
400	5.54	99.92	0.136	-13
300	5.54	99.88	0.189	-15
200	5.54	99.66	0.244	-8
100	5.57	93.18	0.334	16
10	4.74	34.92	0.158	-102
1	6.66	73.58	0.459	169

Wind speed amplitude increases with altitude, from 0.036 m s^{-1} at the surface to 0.334 m s^{-1} in the upper troposphere, consistent with reduced friction at height. Apart from the lowermost layers near the Earth's surface, the phase does not change significantly within the troposphere, indicating that the 6-yr cycle in the zonal winds is almost in phase from the Earth's surface to the tropopause.

https://doi.org/10.5194/egusphere-2026-82
Preprint. Discussion started: 30 January 2026

Next, we extracted the 6-yr cycle of the mean zonal wind speed at the surface and the tropopause, separately averaged over the northern and southern hemispheres. Results are shown in Figure 2.

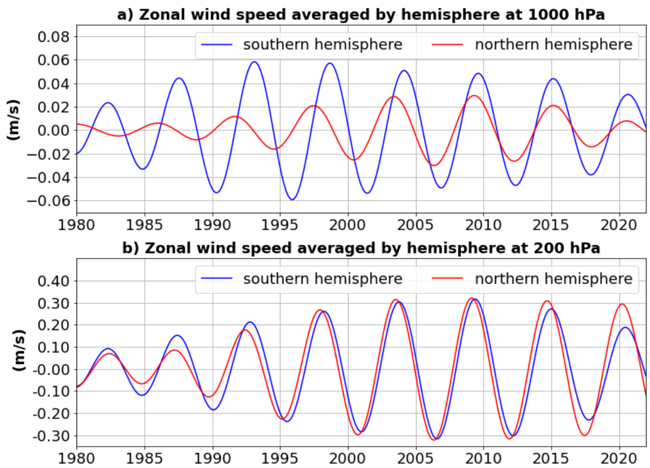

Figure 2. 6-yr cycles over 1980-2022 in the zonal wind speed averaged by hemisphere (southern hemisphere: blue; northern hemisphere: red) a) near the surface (pressure level = 1000 hPa) and b) near the tropopause (pressure level = 200 hPa). The 6-yr cycles were extracted using a fifth-order Butterworth filter with a 5.1 to 7.2-year period band. The zonal wind speed estimates come from the ERA5 reanalysis. Units: m s^{-1}.

From Figure 2, we note that the 6-yr oscillation in zonal wind speed is almost in phase between the two hemispheres. Good phase agreement is noted near the tropopause where the 6-yr cycle has maximum amplitude. At the surface, the cycles start out of phase between both hemispheres and become synchronized later. Early records of the surface zonal wind speed show a weaker amplitude of the six-year cycle in the northern hemisphere, reducing phase significance.

We further analyzed the 6-year cycle in zonal winds as a function of latitude and time using an Hovmöller diagram (Hovmöller, 1949). Figure 3 shows the Hovmöller diagram of the zonal wind speed at the tropopause (200 hPa) as a function of latitude and time.

https://doi.org/10.5194/egusphere-2026-82
Preprint. Discussion started: 30 January 2026

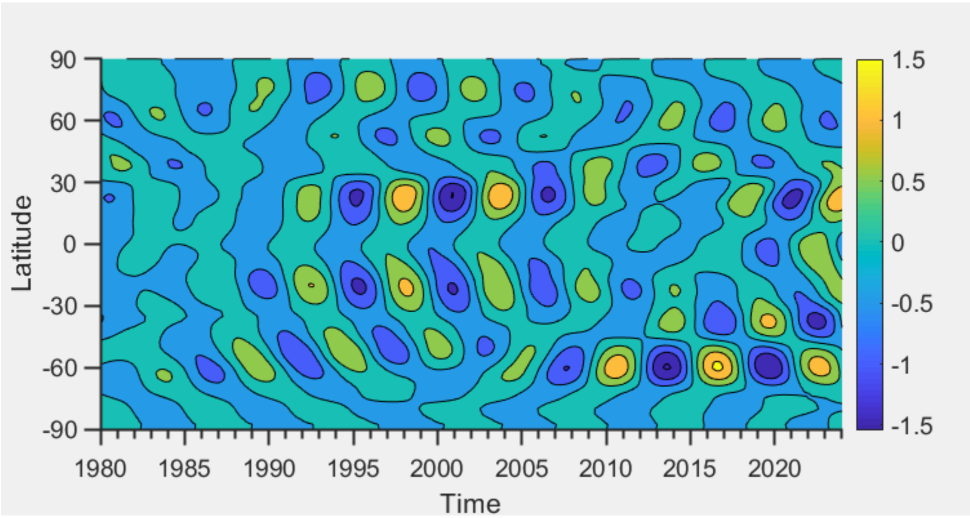

Figure 3: Hovmöller diagram of zonal wind speed near the tropopause (200 hPa) as a function of latitude and time between 1980 and 2024. The 6-yr cycle is extracted using a fifth-order Butterworth filter with a 5.1 to 7.2-year period band. The zonal wind speed estimates come from the ERA5 reanalysis. Units: m s^{-1}.

Figure 3 indicates that the amplitude of the 6-yr cycle in zonal winds is maximum in the tropical region, especially around 30°N/S latitudes. There is slight evidence of propagation from the tropical zone towards the polar regions. Significant 6-yr signal is also observed near 60°S latitudes as of 2010.

Next, we compared the amplitude of the 6-yr cycle in the zonal winds at the Earth surface and near the tropopause with that of the ENSO-related wind and averaged interannual signals. Figure 4 shows the spatial amplitude of zonal-wind variations linked to (a, b) the 6-yr cycle, (c, d) ENSO, and (e, f) interannual variability at 1000 hPa (surface) and 200 hPa (tropopause). The 6-yr cycle amplitude corresponds to the peak-to-trough difference of the band-pass-filtered field (5.1–7.2 years). The ENSO amplitude is derived by regression on the MEI index, and interannual amplitude is estimated from the low-pass-filtered (1.5 yr) field. The 6-yr cycle's contribution to interannual variance (in %) is computed as the relative reduction after removing this component. Figure 4 shows that at the Earth surface, maximum amplitudes for both 6-yr cycle and ENSO-related winds occur over the equatorial Pacific, with secondary maxima near 50° S, 30–50° N, and in the North Atlantic. At the tropopause, maxima of the 6-yr cycle occur in the tropical Pacific (~30° N, 30° S). While the patterns of the 6-yr cycle and ENSO signal were comparable over the Pacific Ocean at the surface, they differ near the tropopause. The 6-

https://doi.org/10.5194/egusphere-2026-82
Preprint. Discussion started: 30 January 2026

yr cycle accounts for 5–25 % of total interannual variance, comparable in magnitude to ENSO but spatially more uniform (Figure 4g).

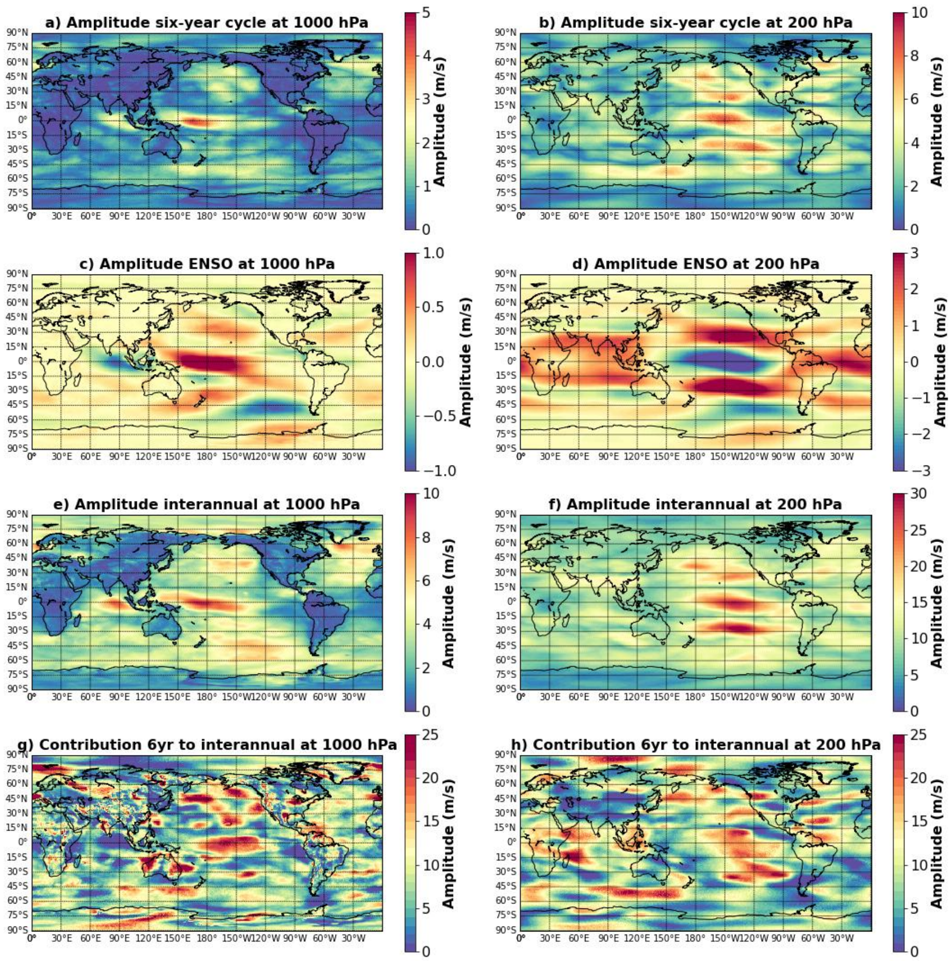

Figure 4: Amplitude of the zonal wind variations at the surface (1000 hPa; panels a, c, e) and near the tropopause (200 hPa; panels b, d, f) for different modes of variability including the 6-yr cycle, ENSO, and interannual variability. The contribution of the 6-yr cycle to the interannual variability of zonal wind speed data (in %) is also shown at 1000 and 200 hPa (panels g, h).

Given that the zonal wind speed variability exhibits distinct latitudinal and altitudinal patterns depending on frequency, the latitude–altitude structure of the 6-yr cycle, ENSO, and interannual variability is shown in Fig. 5. The 6-yr amplitude peaks in the upper troposphere near the equator and at ~50° S, 30° N, and 60° N. In the lower troposphere, maxima appear near 60° S and 60° N, though amplitudes remain small. ENSO-related variability is strongest between 400–100 hPa around 25° N–25° S, whereas the 6-yr mode dominates slightly higher

https://doi.org/10.5194/egusphere-2026-82
Preprint. Discussion started: 30 January 2026

levels. The 6-yr cycle contributes by up to 25 % interannual wind variance at key latitude bands, especially near the equator, 30° N/S, and ~75° N/S, confirming its broad hemispheric coherence.

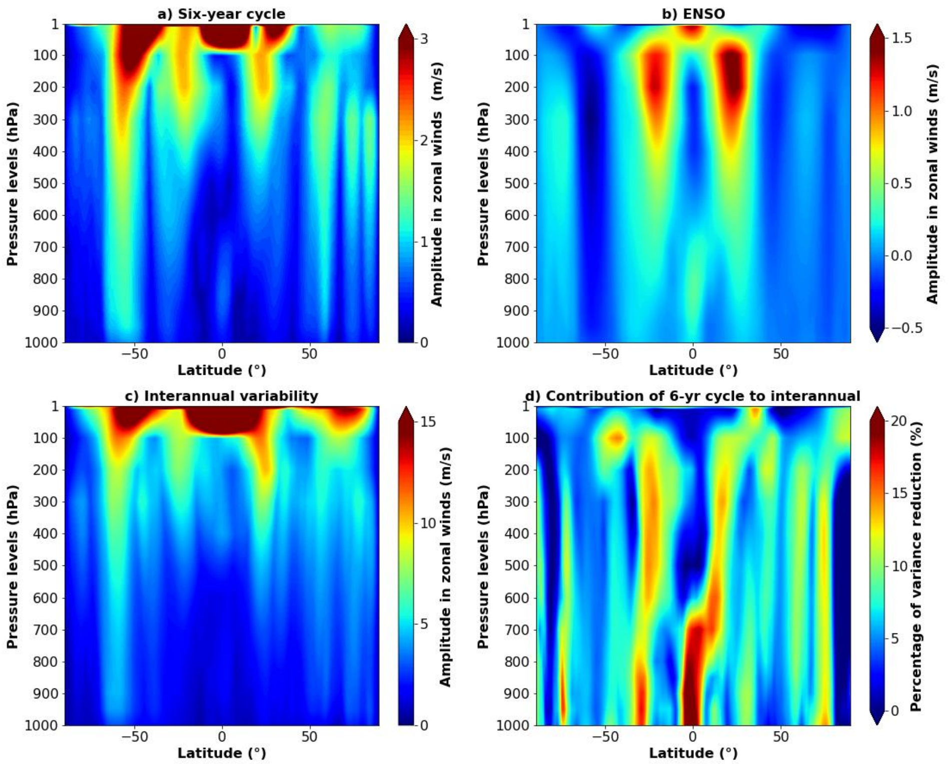

Figure 5: Amplitude of longitude-averaged zonal winds as a function of latitude and altitude for the 6-yr and ENSO cycles (panels a, b). Panel (c)shows the same for the whole waveband of interannual variability, and panel (d) shows the contribution of the 6-yr cycle to the interannual signal.

4. Characteristics of the 6-year cycle in AAM and comparison with LOD

In this section we revisit the 6-yr cycle in the AAM and its relation with LOD. While preliminary results have already been presented in Pfeffer et al. (2023) with wind data from the NCEP/NCAR atmospheric reanalysis, here we also consider two additional wind products (ERA-Interim and MERRA-2 atmospheric reanalyses), in order to validate the NCAR results. AAM 6-yr cycle for the three reanalyses is shown in Figure 6. The LOD 6-yr cycle is superimposed, as well as the LOD corrected for AAM. As previously reported in Pfeffer et al.,

https://doi.org/10.5194/egusphere-2026-82
Preprint. Discussion started: 30 January 2026

(2023), Figure 6 confirms the phase opposition between LOD and AAM starting from the late 1980s, with Pearson correlation coefficients of −0.64, −0.67, and −0.44 for the NCEP, ERA-Interim, and MERRA reanalyses, respectively. The figure also shows that the 6-yr cycle in LOD is amplified after correcting for the AAM.

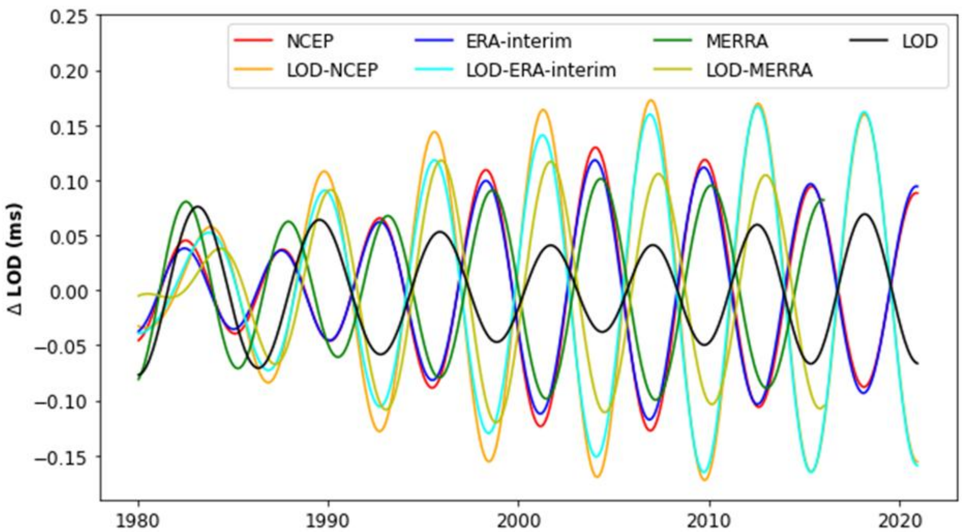

Figure 6: Variations in LOD, AAM, and LOD–AAM time series filtered between 5.1 and 7.2 years (1980–2020). The cutoff periods were selected using the Rayleigh criterion to capture harmonic signals around 6 years. AAM estimates from the NCEP, ERA-Interim and MERRA reanalyses are shown. AAM is expressed in ms (equivalent LOD).

Power spectra of LOD, AAM mass and motion components and LOD minus total AAM for each reanalysis are shown in Figure S1 of the Supplementary Information. These spectra confirm the presence of a quasi-6-yr cycle in LOD, AAM, and LOD–AAM residuals across the three atmospheric reanalyses (NCEP/NCAR, ERA-Interim, and MERRA-2). Corresponding periods and associated confidence levels, as well as amplitudes (expressed in ms equivalent LOD for AAM) are gathered in Table 2. Although the cycle detected in LOD alone shows only moderate significance (confidence level ≈ 68 %), it exhibits an amplitude of 0.086 ms. When LOD is corrected for AAM, the amplitude increases to ≈ 0.11 ms, and the confidence level (CL) rises above 95 %. In contrast, the 6-yr oscillation is highly significant (CL > 99 %) in all AAM series, with consistent amplitudes between 0.076 ms and 0.083 ms. Spectral peaks occur near 5.5 years in AAM and 6.3 years in LOD, while LOD–AAM residuals peak close to 6.0 years. However, these small offsets may not be significant given the limited

https://doi.org/10.5194/egusphere-2026-82
Preprint. Discussion started: 30 January 2026

record length (1980–2020), which restricts frequency resolution according to the Rayleigh criterion. The motion (wind) term dominates the six-year AAM variability, contributing more than 85 % of the total amplitude (see Figure S2 of the Supplementary Information, that shows the 6-yr cycle of the motion and mass components of AAM, as well as their sum, for the three reanalyses).

Table 2: Characteristics of the six-year cycle in LOD, AAM, and, LOD-AAM during the 1980-2020 period. Periods correspond to spectral maxima nearest 6 years. Confidence levels (CL) from red-noise Monte Carlo tests.

Product		**Period (yrs)**	**CL (%)**	**Amplitude (ms)**
LOD		6.29	68.35	0.086
AAM NCEP	**total**	5.49	99.35	0.080
	mass	5.49	99.99	0.010
	motion	5.49	98.95	0.072
AAM ERA-INTERIM	**total**	5.49	99.26	0.076
	mass	5.46	97.76	0.006
	motion	5.49	99.24	0.071
AAM MERRA	**total**	5.46	99.50	0.083
	mass	5.39	99.46	0.014
	motion	5.46	99.20	0.073
LOD – AAM NCEP total		5.99	96.42	0.114
LOD – AAM ERA-INTERIM total		5.99	97.01	0.109
LOD-AAM MERRA total		5.94	95.24	0.108

To quantify the phase and amplitude of harmonic signals near six years, sinusoids with periods between 5.1 and 7.2 years were fitted to the unfiltered series (Figure 7). The largest amplitudes occur at 5.5 years for AAM, 6.3 years for LOD, and 6.0 years for LOD–AAM residuals, consistent with results shown in Table 2. A clear phase opposition between AAM and LOD is observed in the 5.8–6.2-year range. Outside this period band, harmonic signals become less

https://doi.org/10.5194/egusphere-2026-82
Preprint. Discussion started: 30 January 2026

significant, either due to a decrease in amplitude of the AAM (amplitudes not significant for periods longer than 6.2 years) or of the LOD (amplitudes not significant outside the 5.8–6.7 year band). This phase opposition is consistently observed across all three AAM products.

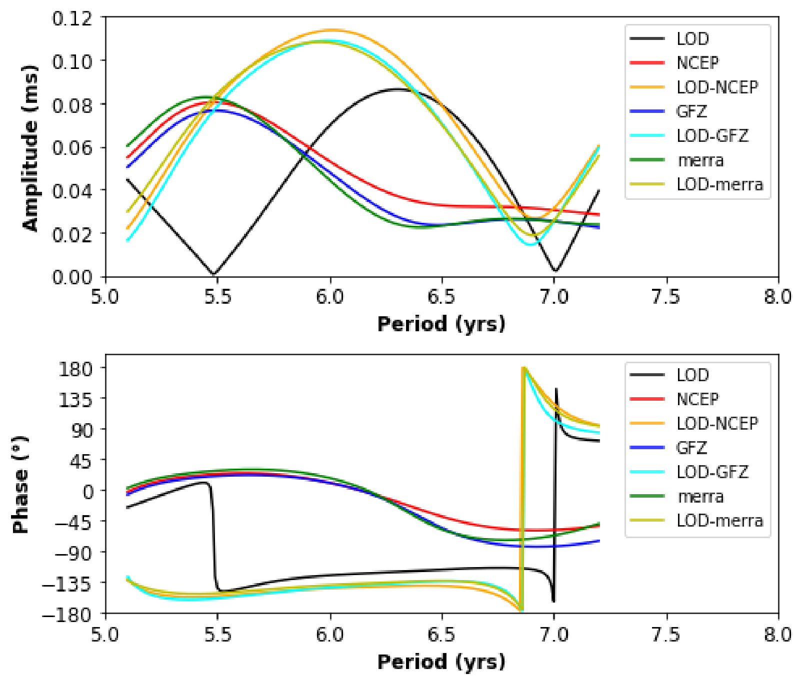

Figure 7: Amplitude (upper panel) and phase (lower panel) of harmonic signals with periods around six years in LOD, AAM, and LOD - AAM time series observed during the common 1980-2016 time span.

5. Discussion

5.1 The 6-yr cycle in the zonal circulation of the atmosphere: a synthesis

The spatial structure of the 6-yr signal detected in the zonal wind circulation was examined using the ERA5 reanalysis, allowing us to identify where variations in zonal-wind speed contribute most to the AAM oscillation. It is found that the signal extends throughout the troposphere up to the tropopause, accounting for 5–25 % of interannual wind variance. Its phase remains consistent between hemispheres, with a maximum signal in the tropical region, and from the surface to the tropopause, indicating a vertically coherent and globally organized circulation pattern. The 6-yr cycle observed in the atmospheric circulation, specifically in

https://doi.org/10.5194/egusphere-2026-82
Preprint. Discussion started: 30 January 2026

zonal wind speed and atmospheric angular momentum, exhibits fundamentally different characteristics from the annual cycle and from known internal climate modes such as ENSO. Its large amplitude and coherent spatial patterns suggest that it represents a distinct mode of variability rather than a simple manifestation of ENSO. Although ENSO has a broad spectral signature that can include periods near six years, its definition through empirical orthogonal functions of climate variability may likely cause elements of the 6-yr cycle to be partially incorporated into the ENSO signal.

The analyses presented above also demonstrate that a quasi-6-yr oscillation in AAM is consistently detected across several independent atmospheric reanalysis products (NCEP/NCAR, ERA-Interim, and MERRA-2) covering four decades, with comparable periods, amplitudes, and phases over the common observational period. This consistency indicates that the 6-yr signal in AAM is unlikely to arise from dataset-specific artifacts and provides a solid observational basis for examining its expression in the zonal circulation and its implications for Earth rotation. The motion term contributes more than 85 % of the total AAM amplitude (0.076–0.083 ms). The oscillation is clearly in phase opposition with the LOD 6-yr cycle. The phase pattern of the 6-yr cycle contrasts with the AAM annual cycle where the zonal wind speeds exhibit phase opposition between the two hemispheres (Lambeck, 1980). For the annual cycle, stronger westerlies (i.e., eastward) winds (especially near the tropopause) occur in the northern hemisphere in boreal winter compared to the southern hemisphere, with the opposite in boreal summer. Consequently, the AAM displays an annual cycle arising from imperfect cancelation in the mean zonal circulation between the northern and southern hemispheres (annual zonal winds being in phase opposition between the two hemispheres). At the 6-yr period, the behavior differs: the oscillation in zonal winds is nearly in phase between the two hemispheres. While LOD shows a weaker but detectable signal (0.086 ms; though only CL ≈ 68 %), after correction for AAM, the amplitude of the 6-yr signal in the LOD residuals increases to about 0.11 ms (CL > 95 %), reflecting the phase opposition between AAM and LOD.

5.2 Link between atmosphere and solid Earth dynamics

To fully understand the variability in LOD at periods around six years, dynamical processes occurring both in the atmosphere and outer core need to be considered. The ensemble of core flow models from Gillet et al., (2022) was analyzed to detect the occurrence, significance, and characteristics of a potential six-year cycle in the core angular momentum (CAM). All ensemble members exhibited power maxima between 5.2 and 6.6 years, with amplitudes

https://doi.org/10.5194/egusphere-2026-82
Preprint. Discussion started: 30 January 2026

ranging from 0.04 to 0.32 m/s (see Figure S3 of the Supplementary Information). The CAM and LOD time series, filtered by a 5th order Butterworth filter covering a period band from 5.2 to 7 years, reveal substantial dispersion in amplitude and phase across core flow predictions, whereas atmospheric estimates are more consistent across reanalyses (Figure 8). The magnitude and phase of the 6-yr LOD cycle suggests that angular momentum transfers from both the atmosphere and outer core contribute to interannual LOD variability.

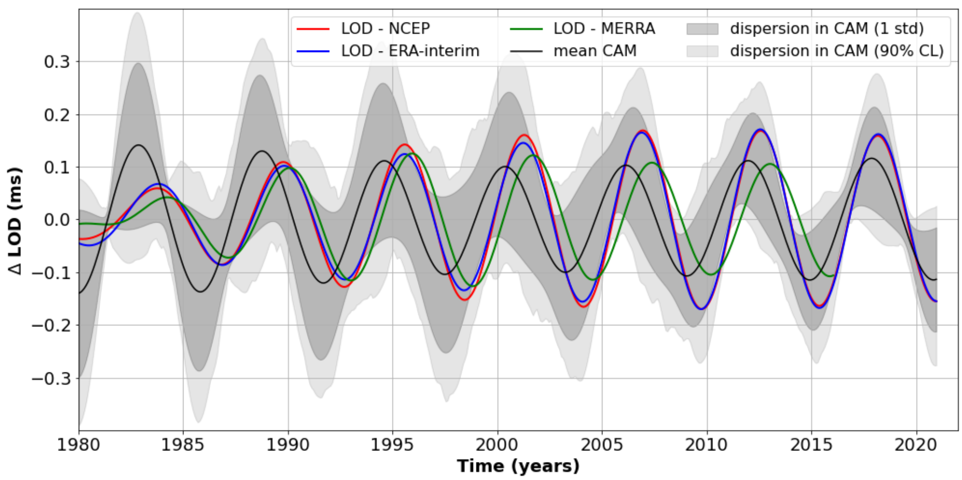

Figure 8. 6-yr cycle predicted from an ensemble of 50 estimates of the core angular momentum (CAM) based on core flow predictions from Gillet et al. (2022). The core flow model dispersion is calculated at 1 standard deviation (dark-shaded area) and 90% (light-shaded area) of the model ensemble. The 6-yr cycle in LOD residuals is also shown, with corrections for the atmospheric contribution estimated with NCEP (red), ERA-Interim (blue), and MERRA (green).

6. Conclusion

The existence of a 6-yr cycle across the Earth system is supported by a broad range of observations (Pfeffer et al., 2023; Cazenave et al., 2025 and references therein). Within the deep Earth, processes operating in the fluid outer core have been shown to exhibit variability at approximately 6–7 years (Gillet et al., 2010; Gillet et al., 2022). A similar 6-yr signal has been identified in the secular variation of the geomagnetic field (Gillet et al., 2022; Lesur et al., 2022; Saraswati et al., 2023). In contrast, evidence for a 6-yr cycle in the climate system has emerged only recently, with oscillations of comparable period reported in several climatic parameters at global and regional scales. In this context, the present study confirms the presence

https://doi.org/10.5194/egusphere-2026-82
Preprint. Discussion started: 30 January 2026

of a 6-yr cycle in the zonal wind circulation and associated atmospheric angular momentum, and documents its spatio-temporal structure.

The relationship between climate variability and deep Earth processes at periods near 6 years nevertheless remains unclear. The two systems may simply exhibit similar periodicities without causal connection. Several possible links have been proposed (Cazenave et al., 2025), including indirect influence of core magnetic field on the climate system, or a common external forcing acting on both climate and core dynamics. Additional hypotheses involve interactions between solid-Earth rotation and atmospheric dynamics, such as modulation of the atmospheric flow through changes in the Coriolis parameter. None of these scenarios have been yet rigorously tested. It is worth noting that the significant peak at 11-12-year signal observed in zonal winds (Figure 1) raises the possibility that the 6-yr oscillation in the atmosphere is a harmonic of this longer period signal, possibly linked to the solar cycle of 11 years. In such a case its origin may be partially or totally disconnected from that of LOD and core motions. Be that as it may, the detailed characteristics of the 6-yr cycle in the atmospheric zonal circulation documented here, including its robustness across several reanalyses and its vertical and latitudinal organization, provide observational constraints that may help discriminate between different scenarios and refine our understanding of how this periodicity manifests across the Earth system.

Data availability

All datasets used in this study are publicly available from the references quoted in the Data and Methods section

Author contributions

JP and AC designed the study. JP and R.A.R analyzed the data. JP and AC wrote a first version of the manuscript. All co-authors contributed to discussing the results, editing and final version of the manuscript.

Competing Interest

The authors declare no competing interest

Acknowledgments

This project has received funding from the European Research Council (ERC) under the European Union's Horizon 2020 research and innovation program (GRACEFUL Synergy Grant agreement No 855677). The FRS-FNRS is acknowledged for supporting the Research Project (PDR No T.0066.20) related to this study. This work has been also funded by ESA in

https://doi.org/10.5194/egusphere-2026-82
Preprint. Discussion started: 30 January 2026

the framework of EO Science for Society, through contract 4000148713/25/NL/FFi (4D Earth Core+). This project was financially supported by CNES as an application of the Swarm mission and GRAVI mission. NG is part of Labex OSUG@2020 (ANR10 LABX56.

References

Barnes, R. T. H., Hide, R., White, A. A. and Wilson, C. A. (1983). Atmospheric angular momentum fluctuations, length-of-day changes and polar motion. *Proceedings of the Royal Society of London. A. Mathematical and Physical Sciences*, *387*(1792), 31-73. https://doi.org/10.1098/rspa.1983.0050.

Bizouard, C., Lambert, S., Gattano, C., Becker, O. and Richard, J.-Y. (2019). The IERS EOP C04 solution for Earth orientation parameters consistent with ITRF 2014. *Journal of Geodesy*, *93*(5), 621-633. https://doi.org/10.1007/s00190-018-1186-3.

Cazenave, A., Pfeffer, J., Mandea, M. and Dehant, V. (2023). ESD Ideas : A 6-year oscillation in the whole Earth system? *Earth System Dynamics*, *14*(4), 733-735. https://doi.org/10.5194/esd-14-733-2023.

Cazenave A., Pfeffer J., Mandea M., Dehant V. and Gillet N. (2025), Why is the Earth system oscillating at a 6-year period? , *Surveys in Geophysics,* 46, 503–528 https://doi.org/10.1007/s10712-024-09874-4.

Chen, J., Wilson, C. R., Kuang, W. and Chao, B. F. (2019). Interannual Oscillations in Earth Rotation. *Journal of Geophysical Research: Solid Earth*, *124*(12), 13404-13414. https://doi.org/10.1029/2019JB018541.

Dee, D. P., Uppala, S. M., Simmons, A. J., Berrisford, P., Poli, P., Kobayashi, S., Andrae, U., Balmaseda, M. A., Balsamo, G., Bauer, P., Bechtold, P., Beljaars, A. C. M., Van De Berg, L., Bidlot, J., Bormann, N., Delsol, C., Dragani, R., Fuentes, M., Geer, A. J., … Vitart, F. (2011). The ERA-Interim reanalysis : Configuration and performance of the data assimilation system. *Quarterly Journal of the Royal Meteorological Society*, *137*(656), 553-597. https://doi.org/10.1002/qj.828.

Dehant V. and Matthews P.M. (2015) Precession, Nutation and Wobble of the Earth, 552 Pages, Cambridge University Press, ISBN: 1-10746582-610746582-6.

Dobslaw, H., Dill, R., Grötzsch, A., Brzeziński, A. and Thomas, M. (2010). Seasonal polar motion excitation from numerical models of atmosphere, ocean, and continental hydrosphere. *Journal of Geophysical Research: Solid Earth*, *115*(B10), 2009JB007127. https://doi.org/10.1029/2009JB007127.

Finlay, C.C., Kloss, C., Olsen, N., Hammer, M. D., Tøffner-Clausen, L., Grayver, A. and

https://doi.org/10.5194/egusphere-2026-82
Preprint. Discussion started: 30 January 2026

Kuvshinov, A. (2020). The CHAOS-7 geomagnetic field model and observed changes in the South Atlantic Anomaly. *Earth Planets Space*, 72, 156. https://doi.org/10.1186/s40623-020-01252-9.

Gelaro, R. et al. (2017). The Modern-Era Retrospective Analysis for Research and Applications, Version 2 (MERRA-2). *Journal of Climate*, *30*(14), 5419-5454. https://doi.org/10.1175/JCLI-D-16-0758.1.

Gillet, N., Huder, L. and Aubert, J. (2019). A reduced stochastic model of core surface dynamics based on geodynamo simulations. *Geophys. J. Int.*, 219(1), 522–539. https://doi.org/10.1093/gji/ggz313.

Gillet, N., Gerick, F., Jault, D., Schwaiger, T., Aubert, J. and Istas, M. (2022). Satellite magnetic data reveal interannual waves in Earth's core. *Proceedings of the National Academy of Sciences of the United States of America*, 119 (13), e2115258119. https://doi.org/10.1073/pnas.2115258119.

Godin, G. (1972). *The analysis of tides*. University of Toronto Press.

Gross, R. S., I. Fukumori, D. Menemenlis and Gegout P. (2004). Atmospheric and oceanic excitation of length-of-day variations during 1980–2000, J. Geophys. Res., 109, B01406, https://doi.org/10.1029/2003JB002432.

Gross, R. S. (2007). Earth Rotation Variations – Long Period, in: Physical Geodesy, edited by T. A. Herring, Treatise on Geophysics, Vol. 11, Elsevier, Amsterdam.

Hersbach, H. et al.(2020). The ERA5 global reanalysis. *Quarterly Journal of the Royal Meteorological Society*, *146*(730), 1999-2049. https://doi.org/10.1002/qj.3803.

Hovmöller (1949), The Trough-and-Ridge Diagram", *Tellus*, vol. 1, no. 2, pp. 62–66, https///doi.org/10.1111/j.2153-3490.1949.tb01260.x.

Huder, L., Gillet, N., Thollard, F., (2019) Pygeodyn 1.1. 0: a Python package for geomagnetic data assimilation. *Geoscientific Model Development*, 12(8), 3795–3803. https://doi.org/10.5194/gmd-12-3795-2019.

Huder, L., Gillet, N., Finlay, C. C., Hammer, M. D. and Tchoungui, H. (2020) COV-OBS.x2: 180 years of geomagnetic field evolution from ground-based and satellite observations. *Earth, Planets and Space*, 72(1), 160, 1–18. https://doi.org/10.1186/s40623-020-01194-2.

IERS Conventions (2010). Gérard Petit and Brian Luzum (eds.). (IERS Technical Note ; 36) Frankfurt am Main: Verlag des Bundesamts für Kartographie und Geodäsie, 2010. 179 pp., ISBN 3-89888-989-6.Istas, M., Gillet, N., Finlay, C. C., Hammer, M. D. and Huder, L. (2023). Transient core surface dynamics from ground and satellite

https://doi.org/10.5194/egusphere-2026-82
Preprint. Discussion started: 30 January 2026

geomagnetic data. *Geophys. J. Int.*, 233(3), 1890–1915. https://doi.org/10.1093/gji/ggad039..

Lambeck, K. (1980) The Earth's Variable Rotation: Geophysical Causes and Consequences. 449 pages, Cambridge University Press.

Pfeffer, J., Cazenave, A., Rosat, S., Moreira, L., Mandea, M., Dehant, V. and Coupry, B. (2023). A 6-year cycle in the Earth system. *Global and Planetary Change*, *229*, 104245. https://doi.org/10.1016/j.gloplacha.2023.104245.

Rekier, J., Chao, B. F., Chen, J., Dehant, V., Rosat, S. and Zhu, P. (2022). Earth's Rotation : Observations and Relation to Deep Interior. *Surveys in Geophysics*, *43*(1), 149-175. https://doi.org/10.1007/s10712-021-09669-x.

Rosat, S. and Gillet, N. (2023). Intradecadal variations in length of day : Coherence with models of the Earth's core dynamics. *Physics of the Earth and Planetary Interiors*, *341*, 107053. https://doi.org/10.1016/j.pepi.2023.107053.

Saraswati, A. T., O. de Viron, and M. Mandea (2023), Earth's core variability from the magnetic and gravity field observations, *Solid Earth*, 14, 1267–1287, https://doi.org/10.5194/se-14-1267-2023.

VanderPlas, J. T. (2018). Understanding the Lomb–Scargle Periodogram. *The Astrophysical Journal Supplement Series*, *236*(1), 16. https://doi.org/10.3847/1538-4365/aab766

Vondrák, J. (1977). The rotation of the earth between 1955.5 and 1976.5. *Studia Geophysica et Geodaetica*, *21*(2), 107-117. https://doi.org/10.1007/BF01634821.

Wolter, K. and Timlin, M. S. (1998). Measuring the strength of ENSO events : How does 1997/98 rank? *Weather*, *53*(9), 315-324.

Zhou, Y. H., Salstein, D. A. and Chen, J. L. (2006). Revised atmospheric excitation function series related to Earth's variable rotation under consideration of surface topography. *Journal of Geophysical Research: Atmospheres*, *111*(D12), 2005JD006608. https://doi.org/10.1029/2005JD006608.

Zhuang, J. et al. (2024). *pangeo-data/xESMF : V0.8.8* (Version v0.8.8) [Logiciel], Zenodo. https://doi.org/10.5281/ZENODO.4294774.

https://doi.org/10.5194/egusphere-2026-82
Preprint. Discussion started: 30 January 2026

Supplementary Information (SI)

Supplementary Information 1

The supplementary S1 contains the power spectral densities calculated for the length of day, atmospheric angular momentum, and residual length of day observations corrected for atmospheric angular momentum. The confidence level corresponds to the percentile of 10,000 red noise models, whose total power and auto-correlation coefficient match those of the considered products.